Double-Frequency Filter Based on Coupling of Cavity Modes and Surface Plasmon Polaritons
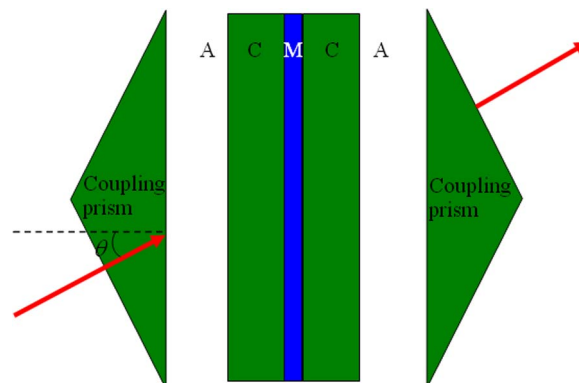
Yun-tuan Fang
Jian-xia Hu
Ji-jun Wang

Double-Frequency Filter Based on Coupling of Cavity Modes and Surface Plasmon Polaritons

Yun-tuan Fang,[1] **Jian-xia Hu,**[1] **and Ji-jun Wang**[2]

[1]School of Computer Science and Telecommunication Engineering, Jiangsu University, Zhenjiang 212013, China
[2]Department of Physics, Jiangsu University, Zhenjiang 212013, China

Abstract: In order to achieve a double-frequency filter, we design a sandwiched structure with a dual-prism total reflection configuration. The sandwiched structure consists of one metal layer and two same media layers. The transmission properties are studied through the standard transfer matrix method. Such system can form two hybrid cavity-surface plasmon–polariton modes. The coupling of the two hybrid modes results in resonance tunneling effect and mode splitting. Mode splitting leads to the coupled double peaks. The difference of double-peak frequencies can be adjusted through changing the metal thickness, and the position of double peaks can be also tunable through changing incidence direction. Such system can be used in designing double-frequency filters and terahertz emission devices.

Index Terms: Double-frequency filter, surface plasmon polaritons, cavity modes, coupling.

1. Introduction

Surface plasmon polaritons (SPPs) are electromagnetic surface state formed on the boundary of metallic and dielectric media, which allow for localization of light on a scale beyond the diffraction limit [1]–[3]. Due to their ability to manipulate light at nanoscale, they are of great importance in many applications such as biosensing [4], surface-enhanced Raman scattering [5], and photonic circuits [6]. The excitation of SPPs is usually based on the use of coupling prism.

On the other hand, the coupling effect in pairing interaction systems could provide many interesting phenomena or potential applications. For example, the phenomenon of strong mode pushing was experimentally observed in coupled semiconductor microcavities [7]; the bonding and antibonding magnetic plasmon modes were theoretically depicted in two coupled split-ring oscillators [8]; the symmetric and antisymmetric combinations of the isolated interface evanescent states were illustrated in two spatially separated Bragg reflectors (BR) [9], and a terahertz (THz) emission device was proposed by Kitada *et al.* [10] based on the GaAs/AlAs coupled multilayer cavity structure. In the configuration from [9], Brand *et al.* studied two evanescently coupled interface states with the use of two prisms overlaid with multilayer dielectric coatings [9]. The evanescently coupled interface states can interact to produce a pair of very narrow transmission lines, the separation of which can be adjusted by varying the size of the gap between the two prisms. In this paper we use the combination
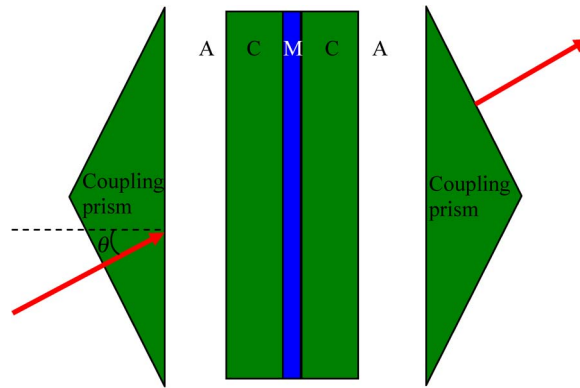
Fig. 1. The schematic of designed symmetric structure, consisting of two coupling prisms and a sandwiched structure C/M/C. The prisms and layers C are made of the same material Si and layer M is made of silver. Two layers A are air gaps. Light is incident on from the prism with the incidence angle.

of a dual-prism system and a sandwiched structure to achieve a hybrid coupled mode from the coupling of SPP and cavity mode. Through the simpler model, we also obtain tunable double frequency resonance peaks.

2. Structure Model and Numerical Results

As shown in Fig. 1, the designed symmetric system is composed of a sandwiched structure C/M/C and two coupling prisms. Two layers C with the same thickness and the prisms are all made of Si with refraction index $n_C = 3.48$. Layer M is made of silver. Two layers A with the same thickness are air gaps. If the incidence angle is larger than the critical angle $\theta_c = \arcsin(1/3.48)$ rad $\approx 16.7°$, the evanescent field will be coupled into the sandwiched structure through the air gap. If the sandwiched structure is replaced by a single layer C, the layer C will become a resonance cavity similar to Fabry–Pérot cavity. In current structure, due to the inserting of layer M, one layer C is split into two layers which may form two cavity modes, and SPPs may be also excited on the two interfaces of metal. The SPPs and cavity modes may be coupled. This coupling will result in a new hybrid resonance mode called as SPP-cavity mode in this paper. The properties of the hybrid resonance mode can be seen from the transmission spectra of structure which can be calculated through the standard transfer matrix method [11]. Such method has been used to study coupling resonant cells, e. g., the formation of split of modes in the prism coupling system [9]. The permittivity for silver can be expressed as Drude Model:

$$\varepsilon_M = 1 - \omega_{ep}^2 / (\omega^2 + i\omega\tau). \tag{1}$$

Here $\omega_{ep} = 1.2 \times 10^{16}$ s^{-1} is the electronic plasma frequency and $\tau = 1.45 \times 10^{13}$ s^{-1} is the damping constant referring to the loss. This choice of ω_{ep} and τ gives a reasonable match to the experimentally determined relative permittivity of silver in the visible part of the spectrum [12]. In order to analyze the coupled mode features, we first consider the ideal case of $\tau = 0$. The thicknesses for all layers are initially chosen as $d_A = 400$ nm, $d_C = 1500$ nm, and $d_M = 50$ nm. Due the coupling effect of SPP and cavity mode, both TE mode (the electric field direction is perpendicular to incidence plane) and TM mode (the magnetic field direction is perpendicular to incidence plane) can excite the coupled resonance. The transmission spectrum at the incidence angle $\theta = 36°$ in the low frequency range is shown in Fig. 2. It is seen that there are some peaks. For TE mode the first and the second are single peak with transmittance smaller than unit, while for TM mode the first is a single peak with transmittance equal to unit. At the first single peak positions of TE mode, the wavelength in layer A (more than 800 nm) is much larger than the thickness of layer A so that light can directly enter into layer C through evanescent field and a cavity resonance in layer C
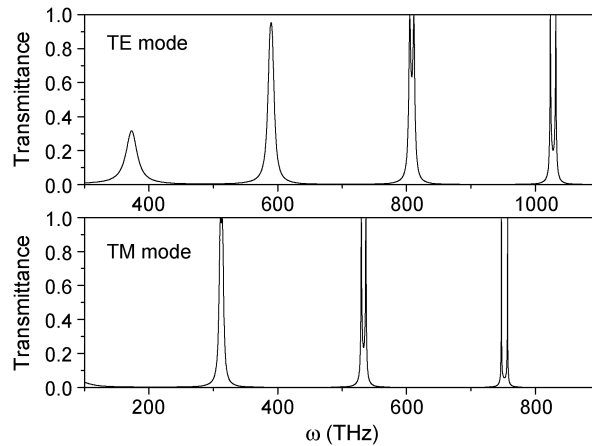
Fig. 2. The transmission spectrum at the incidence angle $\theta = 36°$ in the low frequency range for $d_M = 50$ nm.

can not be formed leading to a non-complete transmission. If we increase the thickness of layer C by steps, we find that the peak value increase accordingly and up to unit, and the single peak will be also split into two sub-peaks. For paper size we do not plot the results. For the latter peaks for both TE mode and TM mode, the clear features are that the single peak is split into two sub-peaks and they both achieve perfect transmission. The reason is that at the smaller wavelengths the cavity mode and SPP have been formed and coupled and the hybrid SPP-cavity resonance has been formed. Due to the symmetrical structure, there are two hybrid SPP-cavity modes. The two hybrid SPP-cavity modes will be further coupled leading to the mode split. Thus a single peak is split into coupled double-peaks. Due the coupling effect and the resonance effect a perfect resonance tunneling occurs. If we remove layers C and the whole structure becomes prism/A/M/A/prism, we find through calculations that the transmittance is small in throughout frequency range considered. This is because that in the configuration of prism/A/M/A/prism, only the coupling of two SPPs has no enough resonance energy to achieve the resonance tunneling. Thus the coupling of cavity mode and SPP play an important role in achieving the tunneling effect. In fact there are a series of peaks corresponding to different orders in the whole frequency range, but all the peak positions for TE mode and TM mode are different. As shown in Fig. 2, for the peaks with lower order the coupled double-peaks are not completely separated. But for the higher order peak the coupled double-peaks are completely separated. Thus we turn to the sixth peak of TE mode which is shown in Fig. 3 (not shown in Fig. 2). The single peak has been split into completely separated double-peaks. The interval of the double-peaks denotes the coupling degree. It can be seen from the figure that the larger frequency, the larger interval of the double-peaks. In the same frequency range, the coupling degree is dependent on the thickness of layer M. Thus we can change d_M to adjust the interval of the double-peaks. The results are also shown in Fig. 3. It is clearly shown that the interval monotonously increases with the decreasing of d_M. The less d_M, the higher the coupling degree. The largest interval for $d_M = 20$ nm is 40.64 THz, while the smallest interval for $d_M = 60$ nm is 7.29 THz. As can be seen, all the transmission peaks are much narrow. For TM mode we can obtain similar results. In the configuration of [9], to obtain the narrow transmission lines, the Bragg reflector coated on the prism must have enough period number (usually more tens) to increase the depth of band gap. Also the narrow perfect transmission lines are dependent on strict symmetric structure. A relative difference of a few percent in the widths of the two layers on each sides will gives rise to a noticeable broadening and effectively halves the value of the transmittance. Thus the standard of the fabrication in [9] must be very high. However, the system in this study is just dependent on a simple sandwiched structure. It is easier to maintain a symmetric configuration in the process of fabrication.
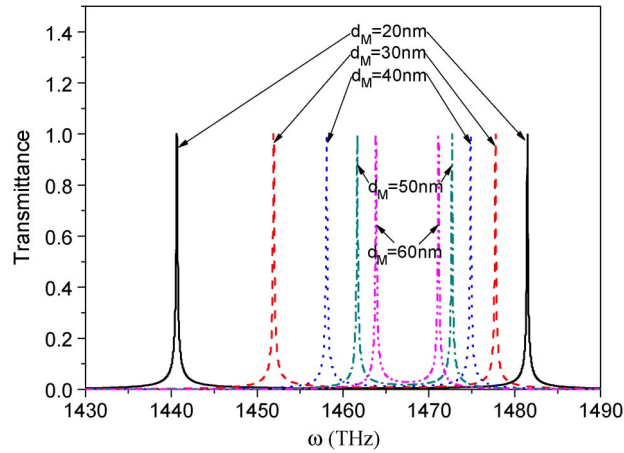
Fig. 3. Double coupled transmission peaks at the incidence angle $\theta = 36°$ for different d_M.

For the double-peaks resulting from the split of mode, we can give an analytical description. A convenient and effective approach is the coupled oscillator model. The hybrid system considered here can be conveniently represented as two coupled oscillators, *i.e.*, two SPP-cavity mode. The eigenenergies of the system can be found by solving the equation [16]

$$\begin{vmatrix} \omega - \omega_0 & \Omega \\ \Omega & \omega - \omega_0 \end{vmatrix} = 0 \qquad (2)$$

where ω_0 are the eigenfrequency of noncoupled SPP-cavity mode and Ω denotes the coupling strength of the two SPP-cavity modes. The value of Ω is dependent on the thickness of metal in current structure. Because of the symmetry structure, the noncoupled SPP-cavity modes have the same eigenfrequency ω_0. Eq. (2) has two solutions

$$\omega = \omega_0 \pm \Omega. \qquad (3)$$

The two solutions just correspond to the two split modes. The value of Ω determines the interval of the double-peaks. The eigenfrequency ω_0 is not fixed which moves to low frequency with d_M decreasing. Thus we find that the shift step of left peak is larger than the right peak in Fig. 3.

To further observe the features of the hybrid SPP-cavity mode, we plot a snapshot in time of the electric field for the coupled double-peaks of TE mode at $\omega = 1461.66$ THz and $\omega = 1472.69$ THz (two green peaks in Fig. 3) corresponding to $d_M = 50$ nm in Fig. 4, respectively. In all the calculations, we assume the incident electric field amplitude is $E_0 = 1$ and the electric field E inside the structure is in unit of E_0. The plots are characteristic of symmetric and antisymmetric coupling of two isolated hybrid SPP-cavity modes. It is seen from the inset that near the two interfaces of layer M the absolute field values undergo decaying within layer M, which takes on the characteristic of SPP. However the absolute field values close to the interfaces from the two sides of layers C do not monotonously decay, which is no longer the feature of SPP. The fields in layers C show the feature of standing waves which is just due to the cavity resonance. Thus the fields close to the metal interfaces from two sides of layers C are modulated by the cavity resonance mode. Fig. 5 further shows the steady-state field patterns at $\omega = 1472.69$ THz corresponding to $d_M = 50$ nm. The fields within layers C are typical characteristics of standing-wave resonance and antisymmetric distribution which is in agreement with the result of Fig. 4 (bottom plot). The standing-wave resonance leads to a great field enhance so that the fields within layers A are too small to be seen. All these just verify our former deduction that there will be a coupling between SPP and cavity mode.

The special transmission spectra of the current structure may be found important applications. First it can be used as double-frequency filters. Only the light with peak frequencies can be
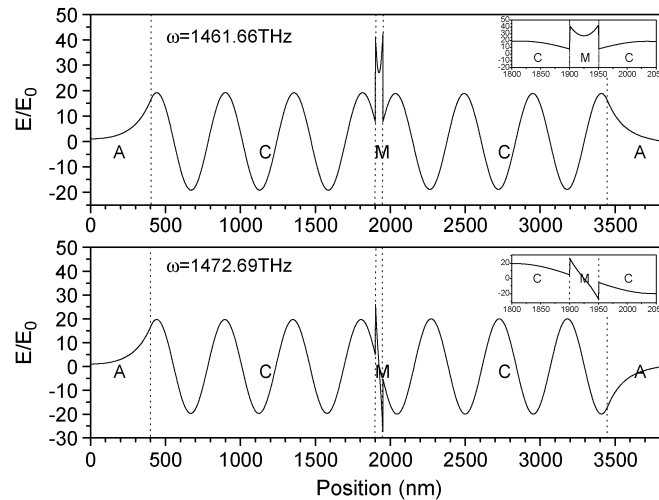
Fig. 4. Snapshot in time of the electric field for the coupled double-peaks at $\omega = 1461.66$ THz and $\omega = 1472.69$ THz corresponding to $d_M = 50$ nm, respectively. The dotted lines denote the interfaces.
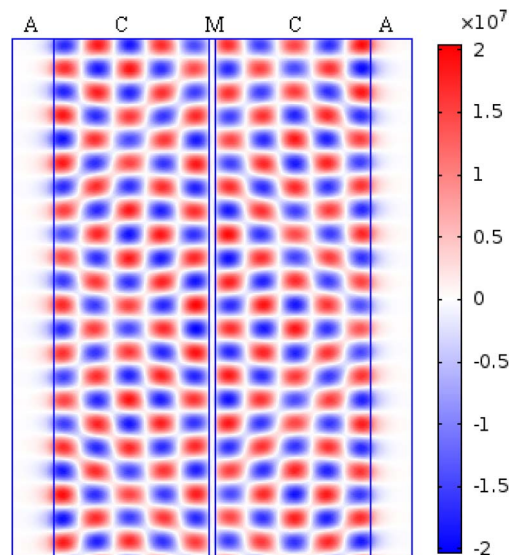

Fig. 5. The steady-state field patterns for the right peak frequency $\omega = 1472.69$ THz corresponding to

transmitted, while other light is reflected. Furthermore, as shown in Fig. 3 the difference frequency of each coupled double-peaks is just in the range of terahertz from several THz to tens of THz. Thus the structure may be found useful in designing terahertz emission devices with the use of difference-frequency generation (DFG) [13]–[15]. In applications, not only the frequency difference can be tunable through changing the metal thickness, but also the double frequency position can be adjusted through changing the incidence angle. Fig. 6 shows the transmission map $T(\theta, \omega)$ of TE mode which is dependent on the incidence angle and frequency. There are two parallel bright curves denoting the double-peaks in the map. It should be noted that the frequency difference of double-peaks has little change, but the double-peak position increases to high frequency with the increasing of incidence angle. Such results help us in designing relevant tunable devices.

Up to now we only consider the ideal case of $\tau = 0$. In real applications, the effect of metal loss can not be neglected. Based on Fig. 3, we calculate the transmission spectra at $\theta = 36°$ for
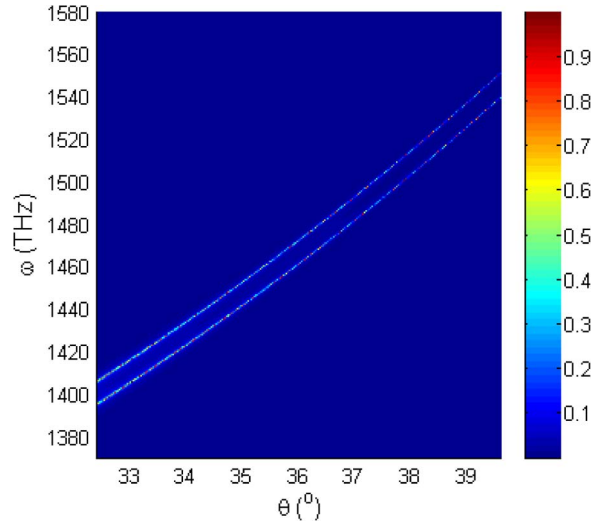
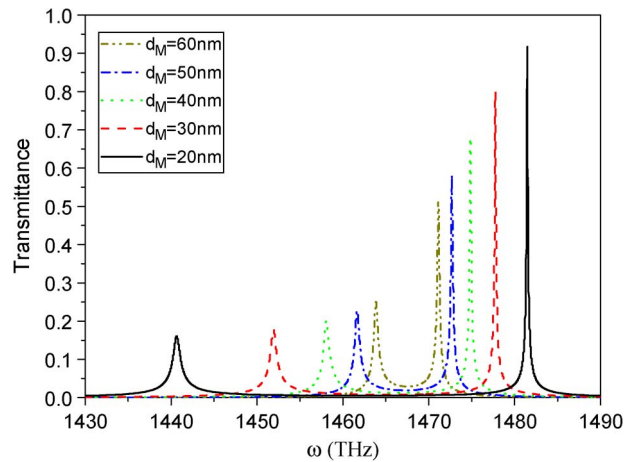Fig. 6. The dependence of the transmission spectra of TE mode on incidence angle and frequency for $d_M = 50$ nm.

Fig. 7. Transmission spectra at $\theta = 36°$ for different d_M with $\tau = 1.45 \times 10^{13}$ s^{-1}.

different d_M but with $\tau = 1.45 \times 10^{13}$ s^{-1}. The results are shown in Fig. 7. From Fig. 7 we find that all the coupled double-peaks still occur at the same positions but with decreased amplitudes. The amplitude of the left peak is always smaller than that of right peak. Moreover, the widths of all the peaks are increased especially for the left peaks. As we know, the broaden peak with low transmittance is not in favor of real application. Because the effect of loss in the low frequency range is larger than that in the high frequency range, to decrease the negative effect, we can turn the position of double-peaks to higher frequency which can be achieved through increasing the incidence angle.

3. Conclusion

In this paper we have designed a sandwiched structure with a dual-prism total internal reflection configuration. Such system is useful in designing double-frequency filter and terahertz emission devices. Compared with other similar structures our designed structure is much simple and easier to be fabricated.

References

[1] W. L. Barnes, A. Dereux, and T. W. Ebbesen, "Surface plasmon subwavelength optic," *Nature (London)*, vol. 424, p. 824, 2003.
[2] R. M. Cole, Y. Sugawara, J. J. Baumberg, S. Mahajan, M. Abdelsalam, and P. N. Bartlett, "Easily coupled whispering gallery plasmons in dielectric nanospheres embedded in gold films," *Phys. Rev. Lett.*, vol. 97, p. 137 401, 2006.
[3] D. K. Gramotnev and S. I. Bozhevolnyi, "Plasmonics beyond the diffraction limit," *Nature Photon.*, vol. 4, p. 83, 2010.
[4] J. Homola, "Present and future of surface plasmon resonance biosensors," *Anal. Bioanal. Chem.*, vol. 377, p. 528, 2003.
[5] A. G. Brolo, E. Arctander, R. Gordon *et al.,* "Nanohole-enhanced Raman scattering," *Nano Lett.*, vol. 4, p. 2015, 2004.
[6] S. I. Bozhevolnyi, V. S. Volkov, E. Devaux *et al.,* "Channel plasmon subwavelength waveguide components including interferometers and ring resonators," *Nature*, vol. 440, p. 508, 2006.
[7] R. P. Stanley, R. Houdré, U. Oesterle, M. Ilegems, and C. Weisbuch, "Coupled semiconductor microcavities," *Appl. Phys. Lett.*, vol. 65, p. 2093, 1994.
[8] H. Liu, D. A. Genov, D. M. Wu, Y. M. Liu, Z. W. Liu, C. Sun, S. N. Zhu, and X. Zhang, "Magnetic plasmon hybridization and optical activity at optical frequencies in metallic nanostructures," *Phys. Rev. B*, vol. 76, p. 073 101, 2007.
[9] S. Brand, R. A. Abram, and M. A. Kaliteevski, "Evanescently coupled interface states in the gap between two Bragg reflectors," *Opt. Lett.*, vol. 35, p. 2085, 2010.
[10] T. Kitada, F. Tanaka, T. Takahashi, K. Morita, and T. Isu, "GaAs/AlAs coupled multilayer cavity structures for terahertz emission devices," *Appl. Phys. Lett.*, vol. 95, p. 111 106, 2009.
[11] P. Yeh, *Optical Waves in Layered Media*. New York, NY, USA: Wiley, 1998.
[12] W. L. Barnes, "Surface plasmon-polariton length scales: A route to sub-wavelength optics," *J. Opt. A: Pure Appl. Opt.*, vol. 8, pp. S87–S93, 2006.
[13] T. Tanabe, K. Suto, J. Nishizawa, K. Saito, and T. Kimura, "Tunable terahertz wave generation in the 3- to 7-THz region from GaP," *Appl. Phys. Lett.*, vol. 83, p. 237, 2003.
[14] T. Taniuchi and H. Nakanishi, "Collinear phase-matched terahertz-wave generation in GaP crystal using a dual-wavelength optical parametric oscillator," *J. Appl. Phys.*, vol. 95, p. 7588, 2004.
[15] I. Tomita, H. Suzuki, H. Ito, H. Takenouchi, K. Ajito, R. Rungsawang, and Y. Ueno, "Terahertz-wave generation from quasi-phase-matched GaP for 1.55 μm pumping," *Appl. Phys. Lett.*, vol. 88, p. 071 118, 2006.
[16] M. Kaliteevski, R. S. Brand, A. Abram, I. Iorsh, A. V. Kavokin, and I. A. Shelykh, "Hybrid states of Tamm plasmons and exciton polaritons," *Appl. Phys. Lett.*, vol. 95, p. 251 108, 2009.